Level structure of ^100Nb

Lhersonneau, G.; Brant, Slobodan; Paar, Vladimir

Source / Izvornik: **Physical Review C - Nuclear Physics, 2000, 62, 44304 - 10**

Journal article, Published version
Rad u časopisu, Objavljena verzija rada (izdavačev PDF)

https://doi.org/10.1103/PhysRevC.62.044304

Permanent link / Trajna poveznica: https://urn.nsk.hr/urn:nbn:hr:217:678494

Level structure of ^{100}Nb

G. Lhersonneau
Department of Physics, University of Jyväskylä, P.O. Box 35, FIN-40351, Jyväskylä, Finland

S. Brant and V. Paar
Department of Physics, Faculty of Science, University of Zagreb, Zagreb, Croatia

(Received 20 April 2000; published 1 September 2000)

Levels in the odd-odd nucleus ^{100}Nb situated at the edge of a region of especially fast shape transitions have been calculated in the framework of the interacting boson fermion fermion model. Levels observed in decay studies can be interpreted in a spherical basis. Low-lying $I^{\pi}=8^{+}$ and 10^{-} states are predicted. Their relationship with the unplaced levels populated with a 12 μs delay after fission is discussed.

PACS number(s): 27.60.+j, 21.10.−k, 21.60.Fw

I. INTRODUCTION

Neutron-rich nuclei with $Z\approx 40$ and $A\approx 100$ are especially interesting for a number of reasons. First, the double shell closures at $Z=40$ and $N=56$ by reinforcing each other turn out to generate an unusual shell strength near ^{96}Zr [1,2]. The shell effects due to the $d_{5/2}$ neutron orbital seem to vanish for the $Z=42$ Mo nuclei [3] but the very recent study of ^{99}Zr decay to ^{99}Nb confirms the persistence of a strong $N=56$ closure also for ^{99}Nb [4].

The second reason is the sudden shape transition between $N=58$ and 60 occurring for Nb and lighter elements. This phenomenon has been related to the rapid lowering of potential energy for a deformed shape with increasing neutron number [5] causing the ground states of the $N=60$ isotones to be strongly deformed, with $\beta\approx 0.30$–0.40 [6–11]. In contrast, Mo isotopes experience a gradual transition, their deformation increasing steadily up to the neutron midshell [12–15]. Therefore, Nb isotopes are located at the high-Z boundary of a region with fast changes. Especially the neutron-rich $N=59$ isotones, located in the transition region, present a challenge for nuclear structure studies. The lowest-lying spherical states in these nuclei, except those in the very neutron-rich nucleus ^{96}Rb observed very recently at the LOHENGRIN recoil separator [16], have been interpreted in the framework of the interacting boson model and its extensions to describe odd and odd-odd nuclei. The interacting boson fermion model (IBFM) was used for the odd-neutron nuclei $^{97}_{38}$Sr [17], $^{99}_{40}$Zr [18], and $^{101}_{42}$Mo [19,20]. The odd-odd nucleus $^{98}_{39}$Y was treated by the interacting boson fermion fermion model (IBFFM) [21,22]. In addition, deformed structures are known to occur near 0.5 MeV excitation energy in ^{97}Sr [17,23,24] and ^{98}Y [25]. The ones expected in ^{99}Zr could not be identified definitely in spite of renewed investigations [26,27]. Surprisingly little experimental data are available for ^{100}Nb, a nucleus very close to the valley of stability, and, to our knowledge, no calculations have attempted so far to describe the presumably complex level structure of this odd-odd nucleus.

We present a calculation for ^{100}Nb using the framework of the IBFFM. It is based on our experimental and theoretical knowledge of the neighboring nuclei. Thus, model parameters will be on the basis of the calculations previously performed to describe the neighboring nuclei. Due to the scarcity of data the present calculation of ^{100}Nb levels can be regarded as a test of the predictive power of the IBM and its extensions. In Sec. II, we review the available data for ^{100}Nb. In Sec. III we present the IBFFM calculations and compare them with available data. We report calculations for both spherical states, for which data exist, and deformed states for which no reliable data are available. Finally, we discuss alternative constructions of the level scheme in an attempt to adjust the available pieces of experimental data in light of our theoretical results. We hope that these calculations will stimulate new experiments which should improve the data collected almost two decades ago.

II. EXPERIMENTAL INFORMATION ON ^{100}Nb

The following information is taken from Nuclear Data Sheets [28]. In Table I the excitation energies of levels in ^{100}Nb observed in beta decay, $(t,{}^{3}\mathrm{He})$ reaction and decay of the 12 μs isomer are displayed (''x'' and ''y'' denote offsets in energy since absolute energies cannot be obtained from these experiments). Decay studies of ^{100}Nb to ^{100}Mo have established the ground state ($t_{1/2}=1.5$ s) as a 1^{+} level from its decay to several ^{100}Mo 0^{+} and 2^{+} states with log ft values below 5.8. Moreover, in ^{100}Nb there is a $I^{\pi}=(4\ \text{or}\ 5)^{+}$ isomer ($t_{1/2}=3.0$ s) at 468 ± 40 keV [29], the energy being obtained from a $Q(\beta^{-})$ experiment. Beta transitions with log ft values suggesting allowed character populate the 4^{+} states at 1136.1 keV (log $ft=5.8$) and 1171.5 keV (log $ft=5.7$), the 6^{+} state at 1846.9 keV (log $ft=5.9$), but also the tentative $I=3$ states at 1607.4 keV (log $ft=5.6$) and 2416.7 keV (log $ft=4.9$). Thus, there is some inconsistency and improvement of the experimental decay scheme is needed to firmly establish the isomeric spin. Nevertheless, the systematics favors the $I^{\pi}=5^{+}$ assignment. In ^{98}Y there is an isomer at 412(40) keV [29], the spin and parity of which have been proposed to be 5^{+} on the basis of its decay properties to ^{98}Zr [30]. Moreover, $({}^{3}\mathrm{He},p)$ reactions have established that in ^{98}Nb the 5^{+} state (84 keV) is lower than the 4^{+} state (226 keV) [30].

A set of ^{100}Nb levels is known from beta decay of ^{100}Zr [31]. The 400.5 and 504.3 keV are clearly 1^{+} states on the basis of their log ft values of 4.8 and 4.4, respectively.

TABLE I. Excitation energies of levels in ^{100}Nb observed in beta decay, $(t,{}^3\mathrm{He})$ reaction and decay of the 12 μs isomer.

Beta decay		$(t,{}^3\mathrm{He})$ reaction	Decay of the 12 μs isomer
E (keV)	I^π	E (keV)	E (keV)
0	1^+	0+x	0+y
400.5	1^+	25+x	34.3+y
468	$(4,5)^+$	131+x	101.7+y
498.0	($\leqslant$3)	210+x	207.6+y
504.3	1^+	348+x	392.8+y
653.9	($\leqslant$3)	410+x	
695.0		450+x	
703.6	($\leqslant$3)	520+x	
		565+x	
		595+x	
		680+x	
		720+x	
		784+x	
		820+x	
		865+x	
		893+x	
		945+x	
		1040+x	
		1075+x	
		1136+x	
		1180+x	
		1260+x	

Other states have $I\leqslant 3$ while their weak feedings do not give information on parity.

In addition, there are levels observed by $(t,{}^3\mathrm{He})$ reaction [32] and another set observed to be delayed with respect to fission by a half-life of 12 μs [33]. The excitation energy of these levels is not fixed with respect to the levels known from beta decay. None of these sets can be matched by shifting the energy scale with the levels known from beta decay in a definite way.

We note that shifting the reaction set upwards by 56 keV produces a very good overlap with the 400, 504, and 654 keV levels and also with the $(4^+,5^+)$ isomer at 468(40) keV. There are, however, several other shifts of higher energy which are equally acceptable from this kind of purely numerical considerations. The decay of the 12 μs isomer was reinvestigated recently by Genevey *et al.* [16]. It is logical to place the isomeric decay scheme on either the 1^+ ground state or the $(4^+,5^+)$ isomer, the latter choice being made by the authors of Ref. [16]. Nevertheless, shifting these levels by 685 keV upwards with respect to the reaction set, we obtain by far the best overlaps of all five levels and even the best overlap of four levels is obtained for a subset of these levels. We may consequently examine the possibility of the existence of a new isomer in ^{100}Nb. This hypothesis is not inconsistent with the scarce data available. A lower half-life limit is set by the fact that the decay of the bottom level of the structure observed at LOHENGRIN has not been observed. Since the time window for coincidences of the impinging ^{100}Nb fission fragments with subsequent gamma radiation was about 20 μs [33] it seems to be conservative to adopt a half-life of at least 50 μs, for which still about 20% of the decays would have occurred within the coincidence window and must have been detected. The upper half-life limit is based on the fact that no new activity has been noticed in detailed decay studies of ^{100}Nb where a gas jet was used to transport the fission products [34]. This gives a somewhat arbitrary limit of a few seconds. Within these limits there remains plenty of room for an isomer to decay without having been noticed.

According to Ref. [28] the 12 μs half-life could be attributed to the highest level at 392.8 keV of the structure observed after fission. This implies very large hindrances of the 185, 359, and 393 keV transitions which depopulate this level. Thus, this isomer could present an analogy with the deformed 495 keV level in ^{98}Y ($t_{1/2}=8.0$ μs) which decays by a 121 keV dipole transition to a spherical level [25]. The alternative interpretation is that the 12 μs isomer is due to the tentatively reported transition of 28 keV [35] if it is placed above the 393 keV level. This transition is confirmed by the experiments by Genevey *et al.* [16]. They establish its placement by coincidence relationships and, in addition, report its $E2$ multipolarity. Thus, the isomer is due to the low energy of the transition rather than to a change of shape between initial and final levels.

Further information from Ref. [35] is the K-conversion coefficient of 4.7(8) measured by the fluorescence method for the 34.3 keV transition. Thus, this is a $M1$ transition with a possible small $E2$ admixture ($\alpha_{K(E1)}=2.3$, $\alpha_{K(M1)}=4.5$, $\alpha_{K(E2)}=28.9$) [36]. Using the experimental half-life of 0.46 μs and correcting for total conversion ($\alpha_{(M1)}=5.1$), we obtain a fairly large hindrance for the $M1$ (2×10^{-4} W.u.) and a small $E2$ collectivity (9 W.u. at 2 standard deviations). It looks therefore improbable that the 34 keV transition is part of a rotational band, although it is still possible that either the initial or final level might be deformed. In contrast, $E1$ multipolarity is reported in Ref. [16] for the 34 keV transition. The authors, however, do not give their experimental conversion coefficient. Thus, the nature of the 34 keV transition remains uncertain.

III. IBFFM CALCULATION FOR ^{100}Nb

The interacting boson model (IBM) of Iachello and Arima [37,38], the interacting boson fermion model (IBFM) [39–41] and the interacting boson fermion fermion model (IBFFM) [42,43] provide a useful framework for description of nuclear structure in even-even, odd-even, and odd-odd nuclei, respectively. The model was further extended by including broken pairs of fermions in the interacting boson fermion plus broken pair model (IBFBPM) [44,45].

During the past decade this framework has been applied to the region of neutron-rich $A\approx100$ nuclei [4,17–22,46–52], which are of particular interest because of an extremely rapid onset of deformation. In this mass region, the IBFM/IBFFM calculations have been performed for ^{96}Y [47], ^{97}Sr [17], ^{97}Y [48,49], ^{98}Y [21,22], ^{99}Zr [18], ^{99}Y [50], ^{99}Nb [4], ^{101}Mo [19,20], ^{101}Zr [51],

and ^{103}Ru [52]. Previous investigations have shown that the ^{98}Y nucleus lies between the lighter nuclei ^{96,97}Y, which exhibit pattern of spherical shell-model states, and heavier nuclei ^{99,100}Y, which exhibit deformed structures with developed rotational bands [21,22,53]. A similar coexistence of spherical and deformed pattern is studied here for the $N=59$ isotone ^{100}Nb.

A. Calculation of spherical states in ^{100}Nb

In the first part of this investigation we have performed the IBFFM calculation of spherical states in ^{100}Nb, by coupling proton and neutron quasiparticles to the SU(5) boson core. This calculation is in analogy to the previous IBFFM calculation of spherical states in the neighboring odd-odd nucleus ^{98}Y [21,22]. Here we employ the same SU(5) IBM core as used in the previous IBFBPM calculation for the neighboring odd-even nucleus ^{99}Nb [4]: $h_1=0.715$ MeV, $h_2=h_3=h_{40}=0$ MeV, $h_{42}=-0.37$ MeV, $h_{44}=0.22$ MeV, with the boson number $N=4$ (the model parameters are defined in accordance with Ref. [54]). We note that this was an effective core, which is between the cores corresponding to ^{98}Zr and ^{100}Mo [4]. Namely, the nucleus $^{98}_{40}$Zr$_{58}$ is magic with respect to the $Z=40$ proton subshell. The first excited 0^+ in ^{98}Zr at 854 keV has a complex particle-hole structure where proton pairs are promoted but the state remains low due to increased proton-neutron interaction. On the other hand, the ^{100}Mo nucleus has two coexisting low-lying structures, approximately associated with O(6) and SU(5) boson systems. Therefore, we have used in the previous ^{99}Nb calculation [4] an effective boson core with $N=4$. This core corresponds to the number of valence shell neutrons. A proton contribution to this effective boson core was not expected to be significant because $Z=40$ is a rather good closed subshell. Furthermore, even if we increase the boson number to $N=5$, because of SU(5) symmetry this increase of boson number could be simulated for low-lying states in the $N=4$ calculation by a small renormalization of core parameters. The proton quasiparticle energies and occupation probabilities are taken from the previous IBFBPM calculation for ^{99}Nb [4]. The $\pi\tilde{f}_{5/2}$, $\pi\tilde{p}_{3/2}$, $\pi\tilde{p}_{1/2}$, and $\pi\tilde{g}_{9/2}$ proton quasiparticle states have quasiparticle energies 1.85, 1.54, 1.37, and 1.04 MeV, and occupation probabilities 0.98, 0.97, 0.92, and 0.13, respectively. The neutron quasiparticles $\nu\tilde{d}_{5/2}$, $\nu\tilde{g}_{7/2}$, $\nu\tilde{s}_{1/2}$, $\nu\tilde{h}_{11/2}$, and $\nu\tilde{d}_{3/2}$, have quasiparticle energies 2.28, 1.56, 1.37, 1.82, and 2.55 MeV, and occupation probabilities 0.93, 0.17, 0.24, 0.11, and 0.06, respectively. They are obtained from the same single particle energies and pairing strength as in Ref. [4]. The boson-fermion interaction strengths for protons are also taken from the IBFM calculation for ^{99}Nb: $\Gamma_0^\pi=0.4$ MeV, $\Lambda_0^\pi=2.5$ MeV, $A_0^\pi=0.02$ MeV [4], and for neutrons from the IBFM calculation for ^{101}Mo: $\Gamma_0^\nu=0.04$ MeV, $\Lambda_0^\nu=1.0$ MeV, $A_0^\nu=0.1$ MeV [20]. The value of the parameter $\chi=-0.5$ has been taken as the average value between the proton and neutron χ values from Ref. [4].

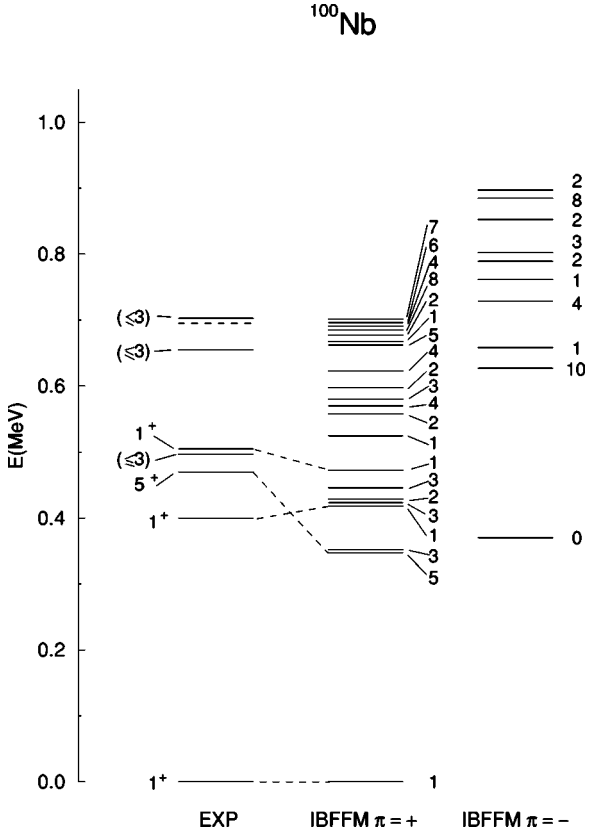

FIG. 1. Spherical states of ^{100}Nb calculated in IBFFM in comparison to the available data.

The strengths of the residual proton-neutron interactions V_δ and $V_{\sigma\sigma}$ were taken in accordance with the previous IBFFM calculations: The value $V_\delta=-0.27$ MeV was determined by requiring that the diagonal matrix element of δ interaction has the same value for the $\pi\tilde{g}_{9/2}\nu\tilde{g}_{7/2}$ two-quasiparticle configuration as in the previous IBFFM calculations for ^{96}Y [47] and ^{98}Y [21,22]. The value $V_{\sigma\sigma}=0.1$ MeV was taken from the previous IBFFM calculation in Ref. [47]. The tensor interaction strength $V_T=0.034$ MeV was adjusted to ^{100}Nb. The main effect of the tensor interaction is to compress somewhat the group of 1_2^+, 5_1^+, and 3_1^+ states. We note that the tensor term with positive interaction strength gives the matrix elements of the same sign as the surface delta interaction. The calculated results for spherical IBFFM states are presented in Fig. 1. Wave functions of the most relevant states are presented in Table II.

Below 0.5 MeV there are three IBFFM 1^+ states, in accordance with experimental data. The 5_1^+ IBFFM state in that energy region is associated with the experimental $(4^+,5^+)$ isomer at 468 keV.

The main components in wave functions of the 1_1^+ ground state and of the 5_1^+ isomer are

$$|1_1^+\rangle = 0.94|(\pi\tilde{g}_{9/2},\nu\tilde{g}_{7/2})1{,}0\ \ 0;1^+\rangle - 0.24|(\pi\tilde{g}_{9/2},\nu\tilde{g}_{7/2})1{,}1\ \ 2;1^+\rangle + 0.20|(\pi\tilde{g}_{9/2},\nu\tilde{g}_{7/2})2{,}1\ \ 2;1^+\rangle + \cdots,$$

TABLE II. Sizable components in the IBFFM wave functions of some low-lying spherical states in ^{100}Nb. Only the components with amplitudes (denoted ξ) larger than 4% are shown. Basis states are denoted by $|(\pi\tilde{j},\nu\tilde{j}')J_{\pi\nu},n_d\,R;J_k^\pi\rangle$.

J_k^π	$\pi\tilde{j}$	$\nu\tilde{j}'$	$J_{\pi\nu}$	n_d	R	ξ	J_k^π	$\pi\tilde{j}$	$\nu\tilde{j}'$	$J_{\pi\nu}$	n_d	R	ξ
1_1^+	$\tilde{g}_{9/2}$	$\tilde{g}_{7/2}$	1	0	0	0.94	4_1^+	$\tilde{g}_{9/2}$	$\tilde{g}_{7/2}$	3	1	2	0.29
	$\tilde{g}_{9/2}$	$\tilde{g}_{7/2}$	1	1	2	−0.24		$\tilde{g}_{9/2}$	$\tilde{g}_{7/2}$	4	0	0	−0.66
	$\tilde{g}_{9/2}$	$\tilde{g}_{7/2}$	2	1	2	0.20		$\tilde{g}_{9/2}$	$\tilde{s}_{1/2}$	4	0	0	−0.54
								$\tilde{g}_{9/2}$	$\tilde{g}_{7/2}$	5	1	2	−0.23
5_1^+	$\tilde{g}_{9/2}$	$\tilde{g}_{7/2}$	5	0	0	−0.39		$\tilde{g}_{9/2}$	$\tilde{g}_{7/2}$	6	1	2	0.21
	$\tilde{g}_{9/2}$	$\tilde{s}_{1/2}$	5	0	0	0.84							
	$\tilde{g}_{9/2}$	$\tilde{s}_{1/2}$	5	1	2	−0.28	4_2^+	$\tilde{g}_{9/2}$	$\tilde{g}_{7/2}$	4	0	0	0.39
								$\tilde{g}_{9/2}$	$\tilde{s}_{1/2}$	4	0	0	−0.71
3_1^+	$\tilde{g}_{9/2}$	$\tilde{g}_{7/2}$	1	1	2	−0.71		$\tilde{g}_{9/2}$	$\tilde{s}_{1/2}$	4	1	2	0.23
	$\tilde{g}_{9/2}$	$\tilde{g}_{7/2}$	3	0	0	0.55		$\tilde{g}_{9/2}$	$\tilde{g}_{7/2}$	5	1	2	0.30
								$\tilde{g}_{9/2}$	$\tilde{s}_{1/2}$	5	1	2	−0.31
1_2^+	$\tilde{g}_{9/2}$	$\tilde{g}_{7/2}$	1	3	0	0.76		$\tilde{g}_{9/2}$	$\tilde{g}_{7/2}$	6	1	2	−0.24
	$\tilde{g}_{9/2}$	$\tilde{g}_{7/2}$	1	4	2	0.37	8_1^+	$\tilde{g}_{9/2}$	$\tilde{g}_{7/2}$	8	0	0	−0.90
	$\tilde{g}_{9/2}$	$\tilde{g}_{7/2}$	5	3	4	−0.20		$\tilde{g}_{9/2}$	$\tilde{g}_{7/2}$	8	1	2	0.39
3_2^+	$\tilde{g}_{9/2}$	$\tilde{g}_{7/2}$	1	1	2	0.41	0_1^-	$\tilde{f}_{5/2}$	$\tilde{d}_{5/2}$	0	0	0	0.33
	$\tilde{g}_{9/2}$	$\tilde{g}_{7/2}$	1	2	2	−0.27		$\tilde{p}_{1/2}$	$\tilde{s}_{1/2}$	0	0	0	0.80
	$\tilde{g}_{9/2}$	$\tilde{g}_{7/2}$	2	1	2	−0.27		$\tilde{f}_{5/2}$	$\tilde{s}_{1/2}$	2	1	2	−0.32
	$\tilde{g}_{9/2}$	$\tilde{g}_{7/2}$	3	0	0	0.66		$\tilde{p}_{3/2}$	$\tilde{s}_{1/2}$	2	1	2	0.26
	$\tilde{g}_{9/2}$	$\tilde{d}_{3/2}$	3	0	0	−0.21							
	$\tilde{g}_{9/2}$	$\tilde{g}_{7/2}$	5	1	2	−0.30	10_1^-	$\tilde{g}_{9/2}$	$\tilde{h}_{11/2}$	10	0	0	0.94
								$\tilde{g}_{9/2}$	$\tilde{h}_{11/2}$	10	1	2	−0.31
2_1^+	$\tilde{g}_{9/2}$	$\tilde{g}_{7/2}$	1	1	2	0.68							
	$\tilde{g}_{9/2}$	$\tilde{g}_{7/2}$	1	2	2	0.36	1_1^-	$\tilde{p}_{1/2}$	$\tilde{s}_{1/2}$	1	0	0	0.81
	$\tilde{g}_{9/2}$	$\tilde{g}_{7/2}$	2	0	0	−0.55		$\tilde{g}_{9/2}$	$\tilde{h}_{11/2}$	1	0	0	−0.20
								$\tilde{p}_{3/2}$	$\tilde{s}_{1/2}$	2	1	2	−0.24
3_3^+	$\tilde{g}_{9/2}$	$\tilde{g}_{7/2}$	1	4	2	−0.74		$\tilde{f}_{5/2}$	$\tilde{s}_{1/2}$	3	1	2	−0.25
	$\tilde{g}_{9/2}$	$\tilde{g}_{7/2}$	3	4	4	−0.23							
	$\tilde{g}_{9/2}$	$\tilde{g}_{7/2}$	5	4	2	0.30	4_1^-	$\tilde{p}_{1/2}$	$\tilde{g}_{7/2}$	4	0	0	−0.84
								$\tilde{f}_{5/2}$	$\tilde{g}_{7/2}$	5	1	2	0.22
1_3^+	$\tilde{g}_{9/2}$	$\tilde{g}_{7/2}$	1	1	2	−0.83		$\tilde{f}_{5/2}$	$\tilde{g}_{7/2}$	6	1	2	0.24
	$\tilde{g}_{9/2}$	$\tilde{g}_{7/2}$	3	1	2	0.41							
							3_1^-	$\tilde{p}_{3/2}$	$\tilde{g}_{7/2}$	3	0	0	0.39
1_4^+	$\tilde{g}_{9/2}$	$\tilde{g}_{7/2}$	1	3	0	−0.34		$\tilde{p}_{1/2}$	$\tilde{g}_{7/2}$	3	0	0	−0.72
	$\tilde{g}_{9/2}$	$\tilde{g}_{7/2}$	1	4	2	0.68		$\tilde{p}_{3/2}$	$\tilde{g}_{7/2}$	4	1	2	−0.25
	$\tilde{g}_{9/2}$	$\tilde{g}_{7/2}$	3	4	2	−0.48							

$$|5_1^+\rangle = 0.84|(\pi\tilde{g}_{9/2},\nu\tilde{s}_{1/2})5{,}0\ \ 0;5^+\rangle - 0.39|(\pi\tilde{g}_{9/2},\nu\tilde{g}_{7/2})5{,}0\ \ 0;5^+\rangle - 0.28|(\pi\tilde{g}_{9/2},\nu\tilde{s}_{1/2})5{,}1\ \ 2;5^+\rangle + \cdots .$$

Thus the 1_1^+ ground state is based on the $(\pi\tilde{g}_{9/2},\nu\tilde{g}_{7/2})J=1^+,2^+,\ldots,8^+$ quasiproton-quasineutron multiplet. We note that this state in ^{100}Nb corresponds to the IBFFM structure of the excited 1_1^+ state at 548 keV in ^{98}Y [21,22].

In IBFFM the 1_1^+ is the lowest lying state, which is in accordance with the parabolic rule [55]. For the $(\pi\tilde{g}_{9/2},\nu\tilde{g}_{7/2})$ multiplet the occupation number is $O=+1$ (both quasiparticles are particlelike) and the Nordheim number $N=\frac{9}{2}-4+\frac{7}{2}-4=0$. Therefore, the parabolic rule predicts that the two-quasiparticle parabola is concave down, with the 1^+ member of the $(\pi\tilde{g}_{9/2},\nu\tilde{g}_{7/2})J=1^+,2^+,\ldots,8^+$ multiplet being the lowest state, having an additional shift downwards due to spin-spin interaction. In accordance with largest components in the IBFFM

wave functions the calculated 1_1^+, 2_1^+, 3_1^+, 4_1^+, 5_2^+, 6_1^+, 7_1^+, 8_1^+ states approximately correspond to the $\pi\tilde{g}_{9/2}\nu\tilde{g}_{7/2}$ two-quasiparticle states. On the other hand, the 4_2^+,5_1^+ IBFFM states approximately correspond to the $(\pi\tilde{g}_{9/2},\nu\tilde{s}_{1/2})J=4^+,5^+$ doublet states. The corresponding Nordheim number is $N=1$, and the parabolic rule predicts that the 5_1^+ state lies below 4_2^+, in accordance with the IBFFM calculation.

This result is in agreement with the experimental observation of an isomeric 5^+ state in ^{98}Y and reproduces the relative positions of the 4^+ and 5^+ states in ^{98}Nb. We therefore assign the isomer as $I^\pi=5^+$. The strong beta decay branch to the 2416.7 keV level in ^{100}Mo ($\log ft=4.9$) suggests that the tentative 3^- assignment has to be replaced by 4^+. This decay looks similar to the decay of ^{99}Zr to ^{99}Nb with $\pi\tilde{g}_{9/2}$ added as a spectator. The log *ft* value suggests that the Mo level should contain a large $(\nu\tilde{g}_{7/2},\nu\tilde{s}_{1/2})$ amplitude. For comparison, the beta decay of the 8^+ isomer of ^{96}Y to the 4390 keV 8^+ state in ^{96}Zr has a log *ft* value of 5.0 [56]. This seems to be characteristic for transitions of the $\nu\tilde{g}_{7/2}$ to $\pi\tilde{g}_{9/2}$ type in this region.

The parametrization for negative parity states is the same as for positive parity, with the exception of $A_0^\nu=0$ MeV, in accordance with Ref. [4]. The lowest calculated negative parity state is 0^-, having the $(\pi\tilde{p}_{1/2},\nu\tilde{s}_{1/2})0^-$ two-quasiparticle state as the largest component (65%). At $\approx$0.25 MeV higher energy lies the calculated high spin state 10^-, having the $(\pi\tilde{g}_{9/2},\nu\tilde{h}_{11/2})10^-$ two-quasiparticle state as the largest component (88%). No experimental data are available on the negative parity spherical states. Therefore, we have placed the lowest 0^- state at the calculated absolute energy with respect to the position of the calculated 1^+ ground state. In this way we obtain the 10^- state at $\approx$0.65 MeV as an isomeric state.

Comparing the energy difference $E(9/2_1^+)-E(1/2_1^-)$ in ^{97}Y (667 keV) and ^{99}Nb ($-$365 keV) with $E(1_1^+)-E(0_1^-)=548$ keV in ^{98}Y, we can estimate the excitation energy of 484 keV for the 0_1^- level in ^{100}Nb. The 498 keV level with a log *ft* value high enough to be of odd parity ($>$6.1) and its only gamma-ray to the 1^+ ground state, could be tentatively identified as the lowest calculated 0^- IBFFM state. Even more tentatively, one of the 654 or 704 keV levels could be a 1^- level of the $(\pi\tilde{p}_{1/2},\nu\tilde{s}_{1/2})$ origin (corresponding to the 1_1^- IBFFM state). The tentative experimental level at 695 keV could also correspond to such a state, expecially because of its 197 keV transition to the 498 keV level which could correspond by analogy to the 119 keV 1^- to 0^- transition in ^{98}Y. Thus, the family of negative-parity spherical states could be tentatively normalized at the energy by 126 keV higher than shown in Fig. 1, placing the calculated 10_1^- state 70 keV above the calculated 8_1^+ state.

Using the IBFFM wave functions the electromagnetic properties of spherical states in ^{100}Nb were calculated. The effective charges and gyromagnetic ratios were taken from the previous IBFM calculation for ^{99}Nb [4] except for the value of χ which is taken from the present calculation for the energy spectrum:

$$e^\pi=1.5,\ e^\nu=0.5,\ e^{vib}=1,\ \chi=-0.5,\ g_l^\pi=1,$$
$$g_s^\pi=0.4\,g_s^{\pi,free}=2.234,\ g_T^\pi=0,\ g_l^\nu=0,$$
$$g_s^\nu=0.7\,g_s^{\nu,free}=-2.678,\ g_T^\nu=0,\ g_R=\frac{Z}{A}=0.41.$$

The only experimentally available half-life is $t_{1/2}(1_2^+)=0.19\pm0.23$ ns, which is in reasonable agreement with the calculated IBFFM value $t_{1/2}(1_2^+)=0.60$ ns.

The 1_2^+ IBFFM state has rather small reduced transition probabilities for decay into the 1_1^+ ground state, $B(E2)=0.0002\ e^2\mathrm{b}^2$, $B(M1)=0.0010\ \mu_N^2$, while the corresponding experimental values are not available.

The calculated decay pattern of the 1_3^+ IBFFM state is in a reasonable agreement with the decay pattern of the experimental level at 504 keV: The experimental branching ratios for decay into the 1_1^+ and 1_2^+ states are $I_\gamma=100$ and $I_\gamma=2.16$, compared to the calculated values $I_\gamma=100$ and $I_\gamma=0.13$, respectively. Assigning the 1_3^+ IBFFM state to the level at 504 keV we predict its half-life of $t_{1/2}=0.002$ ns.

The experimental $J\leqslant3$ level at 498 keV decays into the 1^+ ground state. A similar decay pattern is obtained for the 3_1^+, 3_2^+, 3_3^+, 2_1^+ calculated states which lie in that energy region. Nevertheless, the 2^+ and 3^+ assignments are inconsistent with the sizable experimental β-feeding intensity. A reduction of this β feeding to be in agreement with the hindered character of the transition is rather unlikely since, according to the ^{100}Zr decay data, it implies that feedings by gamma transitions stronger than the one of 197 keV have been overlooked. Consequently, we support the 0^- assignment as mentioned above which makes direct β feeding of first-forbidden character possible, in agreement with the experimental log *ft* value.

B. Calculation of deformed states in ^{100}Nb

The IBFFM calculation of deformed states in ^{100}Nb was performed in analogy to the previous IBFFM calculation of deformed states in the neighboring odd-odd nucleus ^{98}Y [21,22].

We note that in ^{100}Nb (as well as in other $N=59$ nuclei) we cannot apply the simple assumption that the extra 0_2^+ low-lying state in ^{98}Zr or ^{100}Mo generates the second family of levels. In the $N=58$ nuclei ^{96}Sr and ^{98}Zr the 0_3^+ levels near 1.5 MeV are suggested to be the heads of rotational bands similar to the ground-state bands of the $N=60$ nuclei [5,24]. Therefore in $N=59$ nuclei the additional (deformed) family of levels is based on the deformed ground states of $N=60$ core nuclei. This provides a hint for scaling the calculated deformed levels relative to the spherical ones, i.e., the deformed levels should appear at approximately 700 keV or a few hundred keV lower.

In analogy to the previous IBFFM calculations [21,22], the states calculated using the SU(3) boson core are referred to as deformed states.

Here we employ the prolate SU(3) IBM core corresponding to the states in deformed ^{100}Zr nucleus, with parameters

$\alpha=0.307$ MeV, $\beta=0.125$ MeV (defined in accordance with Ref. [57]), and effective boson number $N=5$. This boson number is taken because it is associated with the deformed neighboring ^{100}Zr core nucleus, which has $Z=40$ and ten valence shell neutrons. The value of parameter α was fitted to the experimental 0_3^+ state at 0.829 MeV as the β vibration, and then the parameter β was determined in such a way that the moment of inertia is the same as in the previous IBFM calculation for the $K=5/2$ band in ^{99}Y [50]. The value of the parameter $\chi=-\sqrt{7}/2$ corresponds to the prolate SU(3) core. It should be noted that a drastic sinking of the 2_1^+ state occurs between ^{98}Zr and ^{100}Zr, with the large $B(E2;\ 2_1^+ \rightarrow 0_1^+)$ value in ^{100}Zr (82 W.u.), revealing a sudden change from mainly vibrational to mainly rotational behavior [58]. However, the g.s. rotational band in ^{100}Zr exhibits some deviations from the rotational limit. In particular, the increase of energy with angular momentum is slower than predicted by the $I(I+1)$ formula. Thus, ^{100}Zr can be fitted only approximatively by using the SU(3) IBM limit. We note that some discrepancies between the present IBFFM calculation and experiment may arise due to these deviations of the boson core from the SU(3) symmetry.

We point out to the problem of choosing the deformed core for ^{100}Nb. The nearest deformed nucleus is $^{100}_{40}\mathrm{Zr}_{60}$. However, three additional physical arguments should be taken into consideration. First, the region of $A\approx 100$ nuclei is characterized by an extremely fast phase transition, involving a rapid onset of deformation. Second, some close-lying even-even nuclei are deformed, in particular $^{98}_{38}\mathrm{Sr}_{60}$. In this case, the boson number should be $N=6$. Third, the shell model pattern may rapidly change with the onset of deformation, diminishing gaps between shells, so that the shell closure is less pronounced, which can lead to an overlap of shells causing a further increase of boson number. For these reasons, there is no clear prescription for choosing the core in this case and the effective deformed core may be more complex, leading to computationally prohibitively large configuration space. On the other hand, we have checked that the IBFFM deformed states considered here are not very sensitive to the boson number and the results for $N=6$ are not expected to differ sizably from those for $N=5$, but they would require a sizably more extensive scope of computations. For this reason, we have adopted a smaller boson number, $N=5$. However, it should be kept in mind that a more realistic calculation would require a larger boson number, in particular in future extensions of investigations to the states of higher spins.

In the calculation of deformed states in ^{100}Nb the same quasiparticle energies and occupation probabilities are used as in the calculation of spherical states, with addition of a high lying $\nu\tilde{f}_{7/2}$ quasiparticle of particle-type character ($v^2=0.01$), at the energy 5 MeV above the $\nu\tilde{h}_{11/2}$ quasiparticle, similarly as in the calculation for the ^{101}Zr nucleus [51]. The boson-fermion interaction strengths for protons are obtained by renormalizing the values used in the IBFM calculation for ^{99}Y [50]: $\Gamma_0^\pi=0.46$ MeV, $\Lambda_0^\pi=6.4$ MeV, $A_0^\pi=0$ MeV, and for neutrons are taken as determined by the IBFM calculation for ^{101}Zr [51]: $\Gamma_0^\nu=0.9$ MeV, $\Lambda_0^\nu=4.0$ MeV, $A_0^\nu=0.15$ MeV. The strengths of the residual proton-neutron interactions were taken the same as in the calculation of spherical states. The positive parity deformed states are shown on the left-hand side (LHS) of Fig. 2.

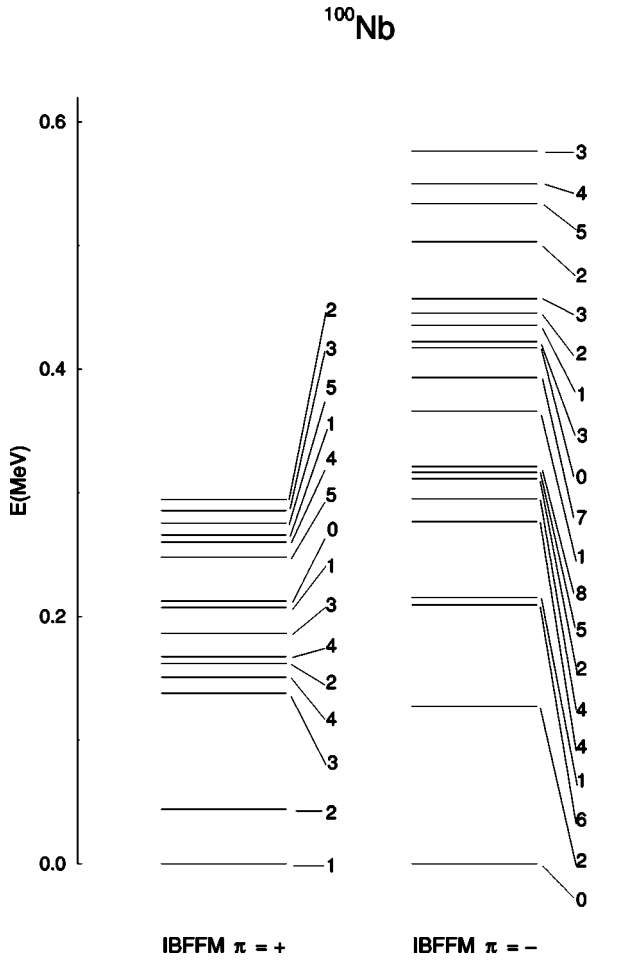

FIG. 2. Deformed states of ^{100}Nb calculated in IBFFM. Both positive- and negative-parity states are not scaled with respect to the ground state (see text).

The interpretation of the IBFFM and IBFM wave functions in terms of Nilsson labels is based on quantitative correspondence of excitation energy, main components in the wave functions and transition probabilities. The interaction strengths in the present calculation reproduce the structure of ^{101}Nb and ^{101}Zr. The lowest calculated band heads in ^{101}Nb correspond to the $\pi[422]5/2$, $\pi[301]3/2$, and $\pi[303]5/2$ Nilsson states at 0, 206, and 208 keV, respectively. In ^{101}Zr the lowest calculated band heads corresponding to $\nu[411]3/2$ and $\nu[532]5/2$ are assigned to the levels at 0 and 217 keV, respectively. In addition, the IBFM calculation predicts in ^{101}Zr a band head at 241 keV, corresponding to the $\nu[413]5/2$ Nilsson state. This structure has not been observed so far. In ^{99}Sr it has been associated with a band built on the 422 keV level [59] but data obtained from β-delayed neutron decay of ^{100}Rb favor the $\nu[532]5/2$ assignment [60].

The lowest calculated positive parity deformed states in ^{100}Nb are 1^+, 2^+, 3^+. These states are based on the

$(\pi\tilde{g}_{9/2}, \nu\tilde{g}_{7/2})$ two-quasiparticle multiplet coupled to the SU(3) boson core. Because of occupation number $O=+1$ and Nordheim number $N=0$, the parabolic rule predicts that the corresponding parabola is concave down, with the 1^+ state being the lowest state, followed by the 2^+ and 3^+ states, in accordance with the IBFFM calculation. The components larger than 4% in the wave function of the lowest 1^+ deformed state contain the $(\pi\tilde{g}_{9/2}, \nu\tilde{g}_{7/2})J_{\pi\nu}$ two-quasiparticle state coupled to bosons in the SU(3) deformed core:

$$|1^+\rangle = 0.26|6,4\ 6;1^+\rangle + 0.29|7,3\ 6;1^+\rangle - 0.27|7,4\ 6;1^+\rangle + 0.21|7,4\ 8;1^+\rangle - 0.29|7,5\ 6;1^+\rangle - 0.32|8,4\ 8;1^+\rangle$$

(with components denoted by $|J_{\pi\nu}, n_d R; 1^+\rangle$).

In terms of Nilsson classification the calculated 1_1^+, 2_1^+, 3_1^+, 4_3^+ states are members of the $(\pi[422]5/2, \nu[411]3/2)$ band with $K^\pi = 1^+$. We note that a similar $K^\pi = 1^+$ rotational band is observed in several other odd-odd nuclei in this mass region (^{100,102}Y, ^{102,104}Nb) [61,62]. The calculated 4_1^+ state is the $K^\pi = 4^+$ head of the same structure. The density of deformed positive parity states is very high due to the presence of several possible configurations at almost same energy.

In the same calculation employing the SU(3) core, the IBFFM calculation provides also the negative-parity deformed states in ^{100}Nb. These states are shown on the RHS of Fig. 2. Due to strong mixing of different components in wave functions and a pronounced staggering, this class of states does not show any distinct band structure. The lowest calculated deformed 0^- state has the main components in the IBFFM wave function containing the $(\pi\tilde{f}_{5/2}, \nu\tilde{d}_{5/2})J_{\pi\nu}$ two-quasiparticle state coupled to bosons in the SU(3) deformed core:

$$|0^-\rangle = 0.20|0,2\ 0;0^-\rangle - 0.41|0,4\ 0;0^-\rangle - 0.22|0,5\ 0;0^-\rangle + 0.24|2,3\ 2;0^-\rangle - 0.43|2,4\ 2;0^-\rangle - 0.20|2,5\ 2;0^-\rangle$$

(with components denoted by $|J_{\pi\nu}, n_d R; 0^-\rangle$). The lowest position of the 0^- negative-parity deformed state is in accordance with the parabolic rule for the multiplet arising from the $(\pi\tilde{f}_{5/2}, \nu\tilde{d}_{5/2})$ two-quasiparticle configuration ($O=+1$ and $N=0$). The wave function of the deformed 0_1^- state shows that it can be associated with the $(\pi[303]5/2, \nu[413]5/2)$ Nilsson configuration and not with $(\pi[301]3/2, \nu[411]3/2)$ which is shifted upwards due to its predominant $(\pi\tilde{p}_{3/2}, \nu\tilde{g}_{7/2})$ structure, with $O=-1$ and $N=0$.

In the absence of any experimental information on deformed states, in Fig. 2 we present the positions of calculated positive- and negative-parity deformed states with respect to the position of the lowest deformed state of each parity.

IV. ALTERNATIVE CONSTRUCTIONS OF THE LEVEL SCHEME

No spin and parities are known for the levels observed in the $(t, ^3\text{He})$ reaction, but they contribute to information on the level density. The 56 keV shift with respect to decay levels allows the best merging of these levels but additional levels at such low energy are not predicted by the spherical IBFFM calculation. An alternative interpretation is that these low-lying levels are deformed. However, this is at variance with systematics of the neighboring $N=59$ isotones (^{97}Sr, ^{98}Y, ^{99}Zr, ^{101}Mo) where, so far, no level below 495 keV (in ^{98}Y) has been claimed to be deformed. Thus, it seems that this good overlap is accidental. A larger shift should restore the level gap in accordance with the IBFFM calculation. A shift of 372 keV only merges the 400 and 504 keV levels with levels from the reaction set. A different shift of 496 keV would not give a match to the 400 keV level, but instead to the 5^+ isomer and the 504 and 704 keV levels. For both of these examples there are extra levels in the reaction data which could represent higher-spin and/or negative-parity levels calculated by IBFFM. However, these states cannot be populated in beta decay of ^{100}Zr. The accuracy of the $(t, ^3\text{He})$ experiment is not sufficient to solve this problem.

The experiments cannot determine the absolute energy of levels observed with a 12 μs delay after fission. The 34 keV transition is not a member of rotational band and there are no spacings clearly indicating rotational structure. Thus, we regard it more likely that some if not all of them belong to the set of spherical states. Since in the IBFFM calculation for spherical levels we obtain a gap of several hundred keV's, it seems to be improbable that the levels of the isomeric decay are placed directly on the 1^+ ground state. Instead, they may be built on the 5^+ isomer or on a new isomer postulated from numerical considerations about excitation energies as mentioned previously. Both assumptions are consistent with the fact that low-lying high-spin levels are predicted by IBFFM. Genevey *et al.* [16] place their levels on the 5^+ isomer and adopt $E1$ multipolarity for the 34 keV transition, resulting in a 8^- 12 μs isomer at about 890 keV. They propose the $(\pi\tilde{g}_{9/2}, \nu\tilde{h}_{11/2})$ configuration since this energy is close to the excitation energy of the $h_{11/2}$ neutron level, as observed in the odd spherical neighbors of ^{100}Nb. In contrast, the IBFFM calculation for spherical states predicts, in agreement with the Nordheim rule, the 10^- state as the lowest-lying for this coupling. This result is independent on details of parametrization. The lowest deformed $(\pi\tilde{g}_{9/2}, \nu\tilde{h}_{11/2})$ IBFFM state is 6^-, followed by 8^- (see Fig. 2) but their relative position is sensitive to details of parametrization. The calculated deformed 6^- is the only state that could be associated with the $E1$ 34 keV transition to the spherical 5^+ isomer. Yet this assignment excludes the deformed 8^- state as a candidate for the 12 μs isomer because both 6^- and 8^- states have the same structure. If the deformed 8^- state is below its 6^- counterpart, there is no candidate for the level that decays by a 34 keV $E1$ transition. The scheme of Genevey *et al.* could be nevertheless interpreted if $M1$ multipolarity is adopted for the 34 keV transi-

tion. In that case, the isomer is a 8^+ state which could be associated with the spherical 8^+ level from the $(\pi\tilde{g}_{9/2}, \nu\tilde{g}_{7/2})$ configuration which is calculated at 0.7 MeV. The intermediate levels between the 8^+ and 5^+ isomers could be then some among a variety of positive parity deformed states predicted by IBFFM.

In the case of a new isomer, one may attempt to interpret the lowest level of the unplaced structure as one of the closely-lying spherical 8^+ or 10^- calculated levels. If the 10^- state is the lowest one, as actually calculated in IBFFM, there is no other decay possibility than beta decay to ^{100}Mo. This decay could be expected to populate the 8^+ and 10^+ yrast states in ^{100}Mo [28]. However, no level with spin larger than 6^+ was reported by Menzen *et al.* [34], which weakens this assumption. Yet it could be that this decay has been overlooked since population of this 10^- level can be only a few percents of the populations of the other 1^+ and 5^+ isomers of ^{100}Nb (see, e.g., the relative populations of the ^{97}Y isomers [63]). On the other hand, if the 8^+ state is the lowest, it could be quite easy to generate an isomeric transition with the half-life fitting in the nondetection range of former experiments. We note that an energy of 0.3 MeV for a $M3$ transition to the 5^+ isomer corresponds to 0.6 s (using W.u.) and such a half-life might already have been causing sizable decay losses in the experiments of Ref. [34].

V. CONCLUSION

This work presents predictions for the level structure of ^{100}Nb, a nucleus situated in a rapidly varying region versus proton and neutron numbers. The calculation for ^{100}Nb in the IBFFM model is based on the results for a number of odd neighbors which were successfully described by the IBFM or IBFBPM calculations and of the odd-odd ^{98}Y described by the IBFFM calculation. The 1^+ ground state is predicted to be spherical and based on the $(\pi\tilde{g}_{9/2}, \nu\tilde{g}_{7/2})$ quasiproton-quasineutron configuration. A large calculated gap for spherical levels above the ground state is followed by two additional 1^+ states which can be assigned to the 400 and 504 keV levels. The calculated 0^- level could be tentatively assigned to the 498 keV level which is weakly fed in beta decay of ^{100}Zr. Higher-lying weakly fed levels could be candidates for the 1^- partner level. This reproduces the level structure seen in beta decay of ^{100}Zr and suggests that the levels observed in $(t, {}^3\mathrm{He})$ reaction lie higher than assumed in the original report. The β-decaying isomer near 470 keV is calculated to be a 5^+ state built on the $(\pi\tilde{g}_{9/2}, \nu\tilde{s}_{1/2})$ configuration.

We note a very good overlap of all levels reported in the decay of the 12 μs isomer with levels from the reaction set if the former are shifted by 685 keV with respect to the latter. This could be a hint to an existence of a new isomer in ^{100}Nb. The 8^+ $(\pi\tilde{g}_{9/2}, \nu\tilde{g}_{7/2})$ or 10^- $(\pi\tilde{g}_{9/2}, \nu\tilde{h}_{11/2})$ configurations are predicted to be in the appropriate energy region and are natural candidates for a potential isomer. Alternatively, this level structure could be placed on the 5^+ isomer, in which case the calculated 8^+ state is a very good candidate for the experimental 12 μs isomer.

In spite of a sudden change of shape from spherical ^{99}Nb to deformed ^{101}Nb, which is very similar to the transition from ^{97}Y to ^{99}Y, there is no experimental evidence for low-lying deformed states in ^{100}Nb, unlike in its lower-Z odd ^{97}Sr and odd-odd ^{98}Y isotones. The calculation for deformed levels, while showing a low-lying 1^+ state which could be populated by allowed β-decay of ^{100}Zr, cannot predict the absolute excitation energy of deformed states with respect to the spherical ones. It might be that these states are lying rather high and, being disfavored by the low decay Q value, their population from ^{100}Zr decay is too weak to have been noticed in experiments carried out with the small detectors available at that time. It should be noted that another open question is the mixing of spherical and deformed states. To this end more information is needed on the overlap between spherical and deformed bosons, which might be small, and the position of deformed set in ^{100}Nb. If these deformed states are sizably shifted up, as proposed in this paper, the mixing of deformed components in the low-lying spherical states will be even smaller.

It is obvious that experimental information is needed to check the validity of the present prediction. Most crucial appears to be a transfer reaction with good energy resolution and determination of l values so that a reliable match between the decay and reaction data sets could be made and some spins and parities be determined. Also of interest would be angular correlation measurements in order to determine the spins of the unplaced levels fed in the decay of the 12 μs isomer, as well as decay studies of ^{100}Nb in order to explore the range of lifetimes between the millisecond and few seconds.

[1] P. Federman, in *Nuclear Structure of the Zirconium Region*, edited by J. Eberth, R. A. Meyer, and K. Sistemich (Springer, Berlin, 1988), p. 357.

[2] G. Molnár *et al.*, in *Nuclear Structure of the Zirconium Region* [1], p. 215.

[3] G. Lhersonneau, B. Pfeiffer, J. R. Persson, J. Suhonen, J. Toivanen, P. Campbell, P. Dendooven, A. Honkanen, M. Huhta, P. M. Jones, R. Julin, S. Juutinen, M. Oinonen, H. Penttilä, K. Peräjärvi, A. Savelius, J. C. Wang, and J. Äystö, Z. Phys. A **358**, 317 (1997).

[4] G. Lhersonneau, J. Suhonen, P. Dendooven, A. Honkanen, M. Huhta, P. Jones, R. Julin, S. Juutinen, M. Oinonen, H. Penttilá, J. R. Persson, K. Peräjärvi, A. Savelius, J. C. Wang, J. Äystö, S. Brant, V. Paar, and D. Vretenar, Phys. Rev. C **57**, 2974 (1998).

[5] G. Lhersonneau, B. Pfeiffer, K.-L. Kratz, T. Enqvist, P. P. Jauho, A. Jokinen, J. Kantele, M. Leino, J. M. Parmonen, H. Penttilä, J. Äystö, and the ISOLDE Collaboration, Phys. Rev. C **49**, 1379 (1994).

[6] C. Thibault, F. Touchard, S. Buttgenbach, R. Klapisch, M. de

Saint Simon, H. T. Duong, P. Jacquinot, P. Juncar, S. Liberman, P. Pillet, J. Pinard, J. L. Vialle, A. Pesnelle, and G. Huber, Phys. Rev. C **23**, 2720 (1981).

[7] H. Ohm, G. Lhersonneau, K. Sistemich, B. Pfeiffer, and K.-L. Kratz, Z. Phys. A **327**, 483 (1987).

[8] R. A. Meyer, E. Monnand, J. A. Pinston, F. Schussler, I. Ragnarsson, B. Pfeiffer, H. Lawin, G. Lhersonneau, T. Seo, and K. Sistemich, Nucl. Phys. **A439**, 510 (1985).

[9] H. Ohm, M. Liang, G. Molnár, and K. Sistemich, Z. Phys. A **334**, 519 (1989).

[10] H. Mach, M. Moszynski, R. L. Gill, F. K. Wohn, J. A. Winger, J. C. Hill, G. Molnár, and K. Sistemich, Phys. Lett. B **230**, 21 (1989).

[11] H. Ohm, M. Liang, U. Paffrath, B. De Sutter, K. Sistemich, A.-M. Schmitt, N. Kaffrell, N. Trautmann, T. Seo, K. Shizuma, G. Molnár, K. Kawade, and R. A. Meyer, Z. Phys. A **340**, 5 (1991).

[12] M. Liang, H. Ohm, B. De Sutter, K. Sistemich, B. Fazekas, and G. Molnár, Z. Phys. A **340**, 223 (1991).

[13] M. Liang, H. Ohm, I. Ragnarsson, and K. Sistemich, KFA-IKP Annual Report 1991, p. 83 (1992).

[14] M. Liang, H. Ohm, B. De Sutter-Pomme, and K. Sistemich, Z. Phys. A **351**, 13 (1995).

[15] H. Mach, B. Fogelberg, M. Sanchez-Vega, A. J. Aas, K. I. Erokhina, K. Gulda, V. I. Isakov, J. Kvasil, and G. Lhersonneau, in *Proceedings of International Workshop on Physics of Unstable Nuclear Beams*, Serra Negra, Sao Paulo, Brazil, 1996, edited by C. A. Bertulani, L. Felipe Canto, and M. S. Hussein (World Scientific, Singapore, 1997), p. 338.

[16] J. Genevey, F. Ibrahim, J. A. Pinston, H. Faust, T. Friedrichs, M. Gross, and S. Oberstedt, Phys. Rev. C **59**, 82 (1999).

[17] G. Lhersonneau, B. Pfeiffer, K.-L. Kratz, H. Ohm, K. Sistemich, S. Brant, and V. Paar, Z. Phys. A **337**, 149 (1990).

[18] S. Brant, V. Paar, and A. Wolf, Phys. Rev. C **58**, 1349 (1998).

[19] H. Seyfarth, H. H. Güven, B. Kardon, G. Lhersonneau, K. Sistemich, S. Brant, N. Kaffrell, P. Maier-Komor, H. K. Vonach, V. Paar, D. Vorkapić, and R. A. Mayer, Fizika (Zagreb) **22**, 183 (1990).

[20] H. Seyfarth, H. H. Güven, B. Kardon, W. D. Lauppe, G. Lhersonneau, K. Sistemich, S. Brant, N. Kaffrell, P. Maier-Komor, H. K. Vonach, V. Paar, D. Vorkapić, and R. A. Mayer, Z. Phys. A **339**, 269 (1991).

[21] S. Brant, V. Paar, G. Lhersonneau, O. W. B. Schult, H. Seyfarth, and K. Sistemich, Z. Phys. A **334**, 517 (1989).

[22] K. Sistemich, O. W. B. Schult, H. Seyfarth, S. Brant, V. Paar, and G. Lhersonneau, Fizika (Zagreb) **22**, 323 (1990).

[23] M. Büscher, R. F. Casten, R. L. Gill, R. Schuhmann, J. A. Winger, H. Mach, M. Moszynski, and K. Sistemich, Phys. Rev. C **41**, 1115 (1990).

[24] J. H. Hamilton, A. V. Ramayya, S. J. Zhu, G. M. Ter-Akopian, Yu. Oganessian, J. D. Cole, J. O. Rasmussen, and M. A. Stoyer, Prog. Part. Nucl. Phys. **36**, 635 (1995).

[25] G. Lhersonneau, R. A. Meyer, K. Sistemich, H. P. Kohl, H. Lawin, G. Menzen, H. Ohm, T. Seo, and D. Weiler, in *Proceedings of the American Chemical Society Symposium on Nuclei off the Line of Stability*, Chicago, 1985, edited by R. A. Meyer and D. S. Brenner, Vol. 324, p. 202.

[26] G. Lhersonneau, P. Dendooven, A. Honkanen, M. Huhta, P. M. Jones, R. Julin, S. Juutinen, M. Oinonen, H. Penttilä, J. R. Persson, K. Peräjärvi, A. Savelius, J. C. Wang, and J. Äystö, Phys. Rev. C **56**, 2445 (1997).

[27] W. Urban, J. L. Durell, W. R. Phillips, A. G. Smith, M. A. Jones, I. Ahmad, A. R. Barnett, M. Bentaleb, S. J. Dorning, M. J. Leddy, E. Lubkiewicz, L. R. Moore, T. Rzaca-Urban, R. A. Sareen, N. Schulz, and B. J. Varley, Z. Phys. A **358**, 145 (1997).

[28] B. Singh, Nucl. Data Sheets **81**, 1 (1997).

[29] G. Audi, O. Bersillon, J. Blachot, and A. H. Wapstra, Nucl. Phys. **A624**, 1 (1997).

[30] B. Singh, Nucl. Data Sheets **84**, 565 (1998).

[31] D. Vogel, Ph.D. thesis, Universität Mainz, Germany, 1982.

[32] F. Ajzenberg-Selove, E. R. Flynn, D. L. Hanson, and S. Orbesen, Phys. Rev. C **19**, 2068 (1979).

[33] E. Monnand, J. A. Pinston, F. Schussler, J. B. Battistuzzi, K. Kawade, H. Lawin, K. Sistemich, and B. Pfeiffer, CEA-N 2176, p. 20 (1980).

[34] G. Menzen, K. Sistemich, G. Lhersonneau, and H. Gietz, Z. Phys. A **327**, 119 (1987).

[35] G. Lhersonneau and K. Sistemich, KFA-IKP Annual Report 1985, p. 29 (1986).

[36] J. Kantele, computer program in *Handbook of Nuclear Spectrometry* (Academic, San Diego, 1995).

[37] F. Iachello and A. Arima, *The Interacting Boson Model* (Cambridge University Press, Cambridge, England, 1987).

[38] A. Arima and F. Iachello, Phys. Rev. Lett. **35**, 1069 (1975); Ann. Phys. (N.Y.) **99**, 253 (1976); **111**, 201 (1978); **123**, 468 (1979).

[39] F. Iachello and O. Scholten, Phys. Rev. Lett. **43**, 679 (1979).

[40] F. Iachello and P. Van Isacker, *The Interacting Boson Fermion Model* (Cambridge University Press, Cambridge, England, 1991).

[41] O. Scholten, Prog. Part. Nucl. Phys. **14**, 189 (1985).

[42] V. Paar, in *Capture Gamma-ray Spectroscopy and Related Topics−1984*, edited by S. Raman, AIP Conf. Proc. No. 125 (AIP, New York, 1985), p. 70.

[43] S. Brant, V. Paar, and D. Vretenar, Z. Phys. A **319**, 355 (1984); V. Paar, D. K. Sunko, and D. Vretenar, Z. Phys. A **327**, 291 (1987).

[44] F. Iachello and D. Vretenar, Phys. Rev. C **43**, 945 (1991).

[45] D. Vretenar, V. Paar, G. Bonsignori, and M. Savoia, Phys. Rev. C **42**, 993 (1990); **44**, 223 (1991).

[46] S. Brant *et al.*, in *Nuclear Structure of the Zirconium Region* [1], p. 199.

[47] S. Brant, G. Lhersonneau, M. L. Stolzenwald, K. Sistemich, and V. Paar, Z. Phys. A **329**, 301 (1988).

[48] G. Lhersonneau, S. Brant, V. Paar, and D. Vretenar, Phys. Rev. C **57**, 681 (1998).

[49] S. Brant, K. Sistemich, V. Paar, and G. Lhersonneau, Z. Phys. A **330**, 365 (1988).

[50] B. Pfeiffer, S. Brant, K.-L. Kratz, R. A. Meyer, and V. Paar, Z. Phys. A **325**, 487 (1986).

[51] S. Brant (unpublished).

[52] S. Brant, V. Paar, D. Vretenar, and R. A. Meyer, Phys. Rev. C **34**, 341 (1986).

[53] K. Sistemich, J. W. Grüter, H. Lawin, J. Eidens, R. Fabbri, T. A. Khan, W. D. Lauppe, G. Sadler, H. A. Selić, M. Shaanan, and P. Armbruster, Nucl. Instrum. Methods **130**, 491 (1975).

[54] J. Timár, T. X. Quang, T. Fényes, Zs. Dombrádi, A. Krasznahorkay, J. Kumpulainen, R. Julin, S. Brant, V. Paar, and Lj. Šimičić, Nucl. Phys. **A573**, 61 (1994).
[55] V. Paar, Nucl. Phys. **A331**, 16 (1979).
[56] M. R. Bhat, Nucl. Data Sheets **82**, 547 (1997).
[57] V. Paar, S. Brant, L. F. Canto, G. Leander, and M. Vouk, Nucl. Phys. **A378**, 41 (1982).
[58] T. A. Khan, W. D. Lauppe, K. Sistemich, H. Lawin, G. Sadler, and H. A. Selič, Z. Phys. A **283**, 105 (1977).
[59] L. K. Peker, Nucl. Data Sheets **73**, 1 (1994).
[60] G. Lhersonneau, B. Pfeiffer, H. Gabelmann, K.-L. Kratz, and the ISOLDE Collaboration, submitted to Eur. Phys. J. A.
[61] F. K. Wohn, J. C. Hill, J. A. Winger, R. F. Petry, J. D. Goulden, R. L. Gill, A. Piotrowski, and H. Mach, Phys. Rev. C **36**, 1118 (1987).
[62] J. K. Hwang, A. V. Ramayya, J. Gilat, J. H. Hamilton, L. K. Peker, J. O. Rasmussen, J. Kormicki, T. N. Ginter, B. R. S. Babu, C. J. Beyer, E. F. Jones, R. Donangelo, S. J. Zhu, H. C. Griffin, G. M. Ter Akopian, Yu. Ts. Oganessian, A. V. Daniel, W. C. Ma, P. G. Varmette, J. D. Cole, R. Aryaeinejad, M. W. Drigert, and M. A. Stoyer, Phys. Rev. C **58**, 3252 (1998).
[63] G. Lhersonneau, D. Weiler, P. Kohl, H. Ohm, K. Sistemich, and R. A. Meyer, Z. Phys. A **323**, 59 (1986).